

A 2-in-1 Switched-Capacitor Inverter for Next-Generation Modular Motors

Zhiheng Luo, Hai-Nam Vu, Ratul Das, and Hanh-Phuc Le

Department of Electrical and Computer Engineering, University of California San Diego

La Jolla, California, USA

{z8luo, h2vu, ratuldas, hanhphuc}@ucsd.edu

Abstract—This paper describes a new 3-phase motor drive inverter suitable for low-voltage high-current modular motors. The inverter features a 2-in-1 combination of a switched-capacitor (SC) step-down converter to reduce the input current delivery losses and a 3-phase inverter with full drive power modulation using only 9 low-voltage switches and 3 capacitors. The flying capacitors of the SC inverter can be partially soft-charged utilizing inductance from the stator. A proof-of-concept prototype of the proposed inverter has been built in order to verify the operation and concepts of the switched-capacitor inverter. The preliminary results, including experiments with a commercial DC motor, confirm the feasibility of the design of the proposed inverter.

Index Terms—Switched Capacitor Inverter, Inverter, Modular Motor Driver, Integrated Modular Machine Drive (IMMD), Permanent Magnet (PM) Machine, Motor Drive

I. INTRODUCTION

The future of both the ground and air transportation systems promises to rely on electrification and be diesel/fossil-free. In order to realize this future, it is crucial to improve the drive power, power density, longevity, and efficiency of the power train in electric vehicles. To increase the drive power while managing the size, electric motor designers have been increasing the applied voltage to 800V and beyond [1]. This increasing supply voltage unfortunately imposes serious stress to a small number of power switches in the 3 phase inverters that could create hot spots with difficulty in heat dissipation and integration with the motor systems. These switches, often implemented with SiC semiconductors, do not benefit from technology advancement for low voltage devices. In addition, winding the high-voltage stators and manufacturing these conventional motors require costly labor-intensive methods or complex machinery. These disadvantages and technical challenges essentially lead to higher costs of manufacturing

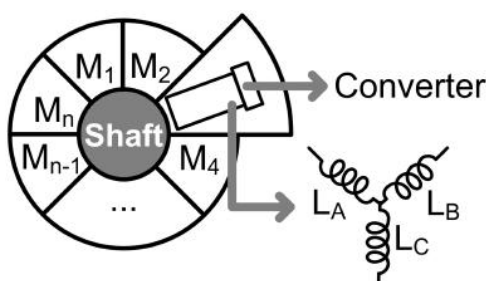


Figure 1: Modular/turn-less motor

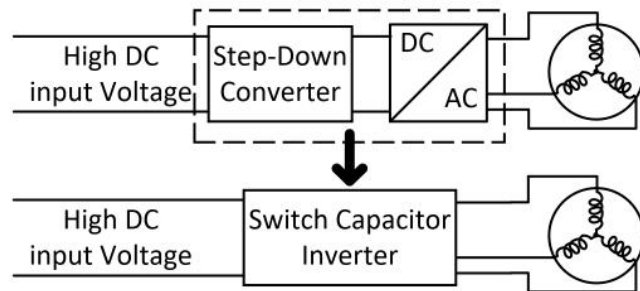


Figure 2: Conventional architecture vs the proposed modular motor drive concept

and ownership. To address these challenges in conventional motors, a turn-less electric motor [2], shown in Fig. 1, has emerged with a novel architecture of multiple low-voltage modular units, each of which is comprised of 3 conductors shorted in a Y configuration to form an active stator and driven by a low-voltage high-current three-phase inverter.

Interestingly, the turn-less motor is similar to the modular motor structure [3] being extensively engineered for electric propulsion motors. A turn-less motor can accommodate many more modules and achieve effective module shedding for power optimization. As the demands for shorter charge time and high efficiency push the battery voltage higher in electric vehicles, low-voltage modules in the motor require efficient and compact point-of-drive converters that can bridge the gap between the high-voltage battery to low-voltage inverters. While this can be done with a step-down converter [4], it is desirable to reduce the number of power delivery stages, active, and passive devices in the power delivery circuitry for higher efficiency, lower complexity and cost.

In this work, a switched-capacitor (SC) inverter is proposed and demonstrated that combines both point-of-drive step-down conversion and 3-phase inversion functions in one synchronous structure conceptually shown in Fig. 2. The compact SC inverter can enable integration with each motor's module in the future [5]. The topology and operation of the proposed inverter will be presented in Section II below.

II. 2-IN-1 SWITCHED-CAPACITOR INVERTER

A. Topology and Operation

As an alternative to the multiple stacked inverters for high input voltage in [6] where a high DC bus voltage is equally

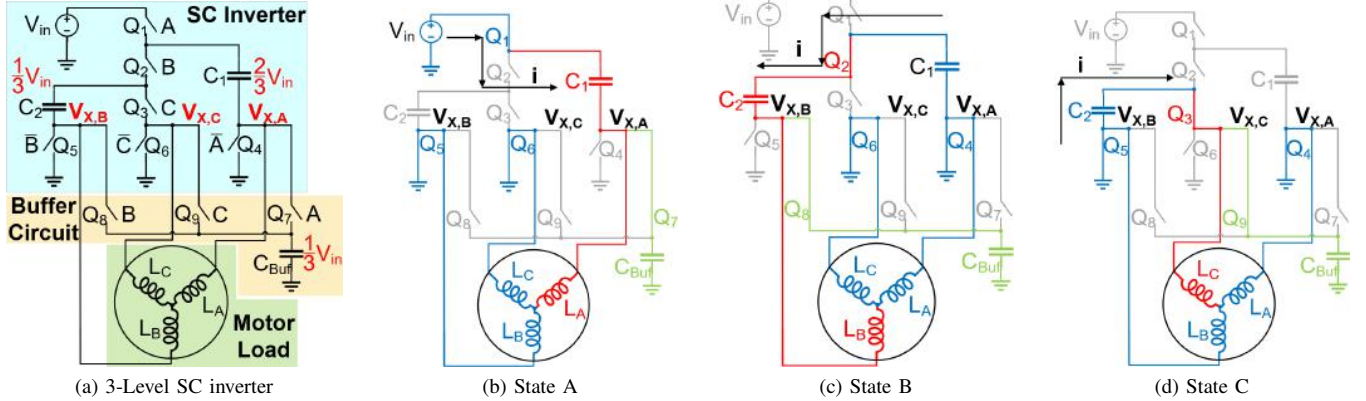


Figure 3: The proposed 3-Level switched-capacitor inverter schematic and its operating states. Active path: charge (red), discharge (blue) and buffer circuit (green).

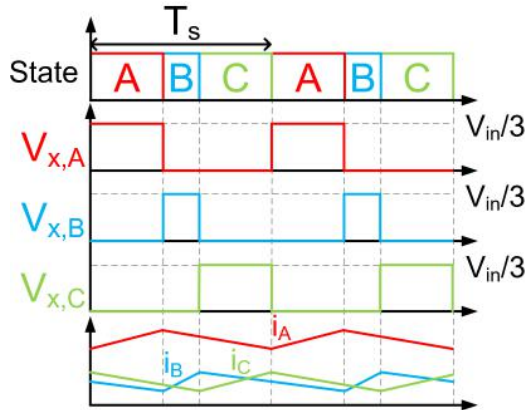


Figure 4: Timing diagram of an example 3-phase operation.

stepped down by DC-link capacitors connected in series for each unit, the proposed inverter uses a merged multi-level SC stage to bring the voltage down before the inversion. The modular 2-in-1 point-of-drive (PoD) inverter features parallel distribution and management to individual 3-phase drive units, improving stability and reliability of the motor especially in phase/module-shedding for optimized operations or in a fault shutdown and bypass at module or multiple module levels without significantly impacting the continuous operation of the system.

The proposed inverter, shown in Fig. 3a, has an integrated 3-level SC structure (for $V_{in}/3$ division) which can be extended to a higher number of levels to support larger voltage conversion requirements [7]. The inverter uses 9 switches, Q_{1-9} , and 2 flying capacitors, C_1 , C_2 and one buffer capacitor C_{Buf} . Switches $Q_{1,4}$, $Q_{2,5}$ and $Q_{3,6}$ construct three half-bridge branches with Q_1 and Q_4 and Q_2 and Q_5 coupled via two flying capacitors, C_1 and C_2 , respectively. Assuming small voltage ripples on the flying capacitors, these SC half-bridges work the same as the half-bridges of conventional 3-phase inverters and can be controlled with the conventional sine PWM (SPWM) technique [8]. Using SPWM, the switching nodes $V_{x,A-C}$ behave the same as the switching nodes of

conventional inverters with an additional voltage stepped-down thanks to the multi-level SC structure. In this SC inverter, the switching node voltages swing between $\frac{V_{in}}{3}$ and 0 [7], [9]. The three inverter branches can be controlled to share the full switching period T_s with the three states A, B, and C and the corresponding schematics in Fig. 3, as shown in the timing diagram in Fig. 4.

The SC inverter can work without the buffer circuit comprised of Q_{7-9} and C_{Buf} . As shown in Fig. 3, the inverter gets charge from the input at the beginning of each switching period in State A, then the charge shuffles through the flying capacitors C_1 then C_2 while charging the rotor winding currents i_A , i_B , and i_C in States A, B, and C, respectively. For example, in phase A as shown in Fig. 3b, neglecting the existence of the buffer circuit, the current of the winding A (L_A) gets energized by the source through Q_1 and the flying capacitor C_1 while the other two winding of the motor (L_B and L_C) discharge to the ground through Q_5 and Q_6 . The winding currents $i_{A,B,C}$ fully soft-charge and soft-discharge the flying capacitors. An additional L-C filter could be added in concern of high-frequency noise injection into the motor windings [10].

B. Buffer Circuit

While the motor currents are switched at high switching frequency, their phase (A, B, and C) duty cycles are modulated following SPWM at a motor electrical frequency. As a result, the currents through the motor windings are sinusoidal and phase-shifted 120° from each other. Depending on the position in the electrical period, charges taken from one of the legs outweighs the others. Therefore, the flying capacitors have charge balance in the electrical period but not the switching period. In other words, without the buffer circuit, C_1 and C_2 would need to handle both motor currents electrical frequency and inverter switching frequency. While their voltages only have small ripples at a high inverter switching frequency of 10s kHz, a low electrical frequency of 10s Hz for the mechanical operation of the motor would cause a large voltage fluctuation on the capacitors for requiring very large capacitance for

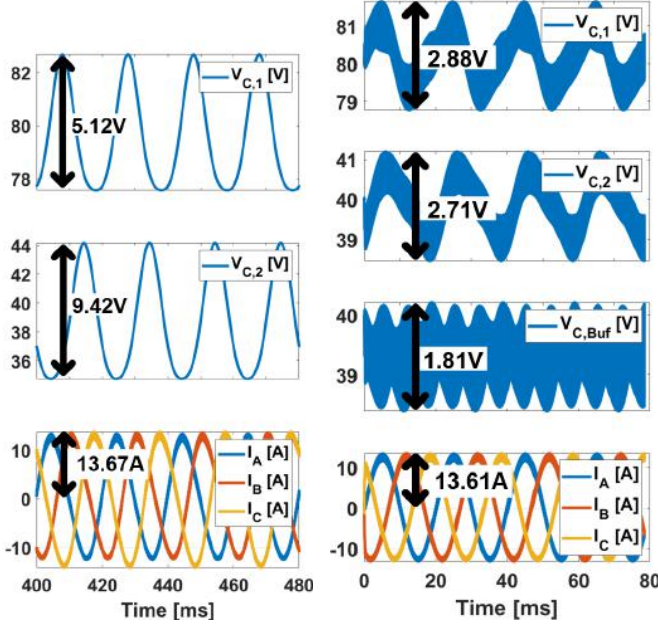
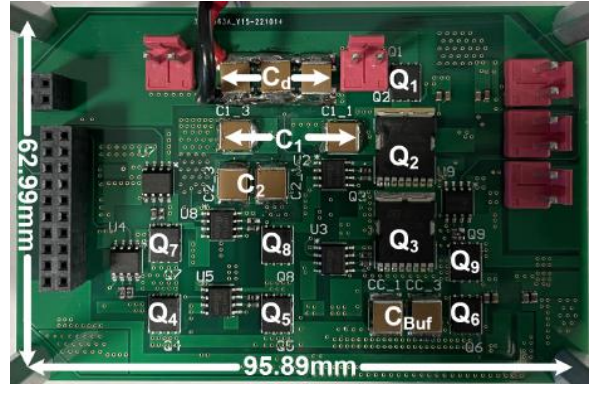


Figure 5: Simulation of $V_{C,1-2}$, $V_{C,Buf}$ ripples and I_{A-C} at 50 Hz electrical frequency

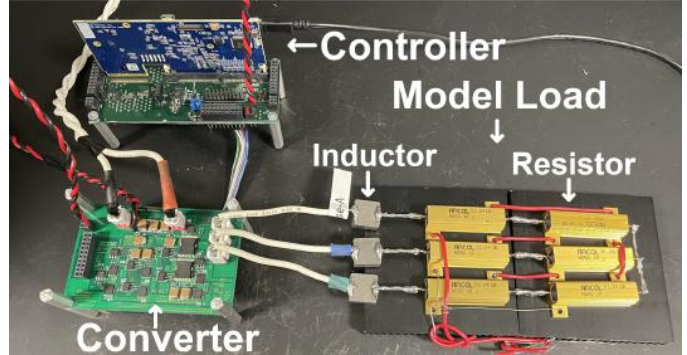
stable operations, especially for a high-power high-current drive application. Fig. 5a illustrate this behavior with large voltage fluctuations on V_{C1} and V_{C2} even with relatively a large capacitance of 500 μ F.

To avoid large capacitors, an additional buffer circuit is added and operated at the inverter switching frequency to maintain continuous charge balance among the three legs at the inverter switching frequency, enabling a significant size reduction for all capacitors. Fig. 5b illustrates the effect of the buffer circuit in significantly reducing the voltage ripples while minimizing values of C_1 and C_2 to only 10.5 μ F, and C_{Buf} to 30 μ F, equivalent to 20X reduction in total capacitance. Compared with six switches of the conventional inverter with no step-down capability, adding three switches and a small capacitor in the buffer circuit is justified to provide both voltage conversion and inversion with small capacitors.

During each phase, the flying capacitors are connected in parallel with the buffer capacitor respectively in AC. Therefore, with the buffer capacitor designed to be at least 3 times bigger than the flying capacitors, the flying capacitors receive compensated charges stored in the buffer circuit from the other two phases. For example, in an electrical period when the current i_A is at its peak value and a lot larger than the other two currents ($i_A \gg i_B \cong i_C$), at the inverter switching frequency, i_A draws a smaller and average current from C_1 and V_{in} while its larger portion comes from the buffer capacitor C_{Buf} that receives the charge surplus from Phases B and C with low i_B and i_C currents utilization from the motor. This way, the two flying capacitors work with the buffer capacitor to re-distribute



(a) Designed prototype



(b) With model loads of 47uH inductors and 2Ω resistors

Figure 6: Prototype and the test setup

Table I: List of Components

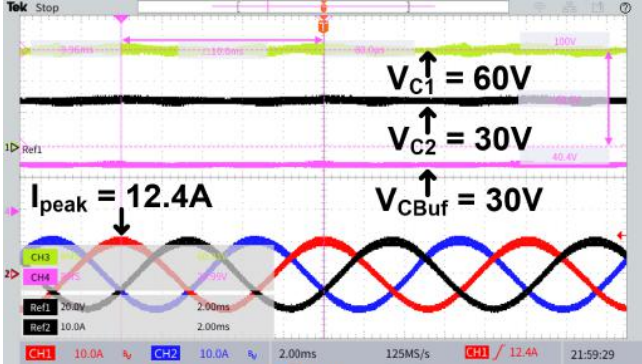
Components	Parts
$S_{2,3}$	600V MOSFET (STMicroelectronics) STO67N60DM6
$S_{1,4-9}$	120V MOSFET (Infineon) BSC110N15NS5ATMA1
$C_{1-2,Buf}$	12x, 7x, 32x 250V 2.2 μ F X7T (TDK)
C_d	6x 450V 2.2 μ F X6S (TDK)
Gate driver	Isolated IGBT Driver (Infineon) 1EDI05I12AFXUMA1
Driver supplies	Isolated DC-DC Converter (Murata) NKE0515SC

the charge to the 3-phase motor unit according to the operation and SPWM control.

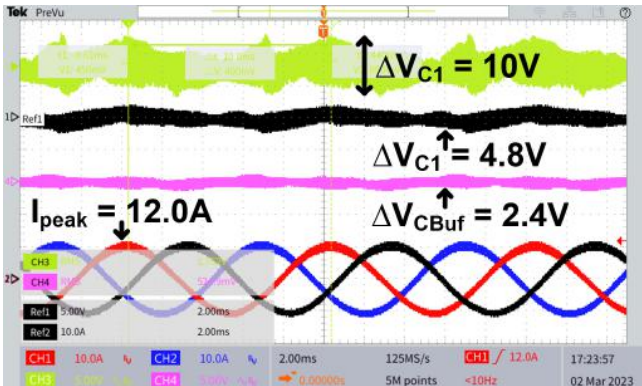
While enabling significant reduction of capacitor values and size, the buffer circuit inevitably introduces hard switching losses during charge sharing between flying capacitors and the buffer capacitor. In the current design and implementation, the additional hard switching loss is about half of the conduction loss of the inverter without the buffer circuit. This loss can be designed and optimized according to the allowed size, capacitor values, and output current capabilities.

Table II: Result Comparison

	Integrated Single-Stage Driver [12]	2-in-1 Switched-Cap. Inverter
Bus Voltage	48V	90V
Addit. Inductor	350uH	0
Switching Freq.	20kHz	100kHz
Efficiency (80W)	94%	90.47%

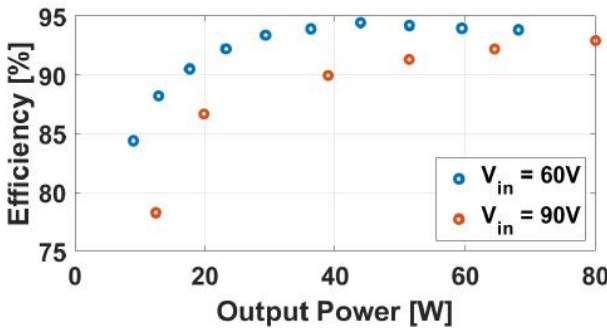


(a) $V_{C,1-2}$ and $V_{C,Buf}$ DC biasing

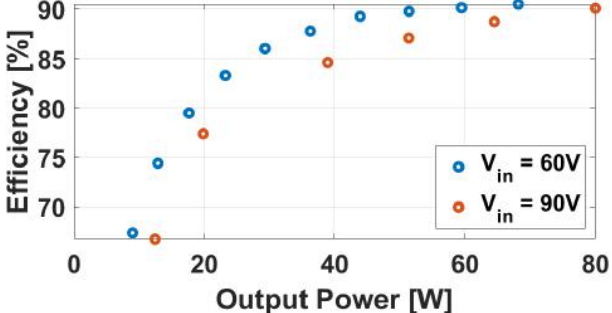


(b) $V_{C,1-2}$ and $V_{C,Buf}$ AC biasing

Figure 7: I_{A-C} , $V_{C,1-2}$ and $V_{C,Buf}$ at $V_{in} = 90V$ at electrical frequency 100Hz



(a) Power stage efficiency



(b) Overall efficiency w/ gate driving losses

Figure 8: Measured performance of the SC inverter prototype

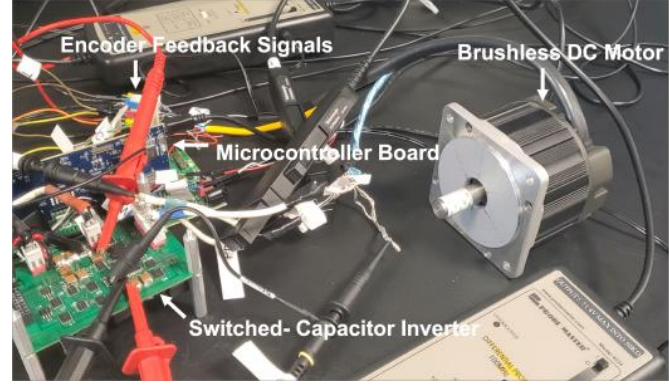


Figure 9: Prototype being tested with Brushless DC Motor

III. EXPERIMENTAL RESULTS

A. Dummy Motor

The prototype shown in Fig. 6a has been designed using the components listed in Table I to verify the operation and concepts of the proposed 2-in-1 SC inverter. The prototype is first tested with a motor model load [11] that is composed of 3 sets of inductors and resistors connected in a Y configuration as shown in Fig. 6b. As recorded in Fig. 7, the SC inverter is operated with 90V DC input, generating 3-phase AC output currents that peak at $\sim 12.4A$. Capacitors C_1 , C_2 , and C_{Buf} maintain their voltages around 60V, 30V, and 30V, respectively, as expected from their operation described in Section II. The SC inverter performance is measured in Fig. 8, achieving a peak power stage efficiency of 94.45% at 43.92W output power, and a peak overall efficiency, including all gate driving losses, of 90.47% at 68.18W output power from a 60V input. The result is compared with the conventional two-stage design [12] presented in Table II.

B. Commercial Motor

The prototype has been tested and verified with a commercial brushless DC motor (part number: M-3411P-LN-08D) as shown in Fig. 9. To drive the motor, a comprehensive motor control was implemented using a micro-controller's functions to read the motor's position and speed based on the motor's encoder feedback signals. Accordingly, the control PWM signals were generated following the sine-wave commutation method to operate the SC inverter to drive the motor. In addition to testing with the commercial motor, another functional verification experiment was also successfully carried out with a 3-wire model of a turn-less motor unit module [2].

IV. CONCLUSION

In summary, a switched-capacitor inverter is proposed that merges the step-down conversion and inverting stages in a single-stage inverter for turn-less or modular motor driving applications. The proposed inverter operation has been verified with a proof-of-concept hardware prototype. Details about the design, operation, measurement results with a dummy motor and verification with a commercial motor are presented to exhibit a promising candidate for power delivery and management of emerging turn-less or modular motors.

ACKNOWLEDGEMENT

This work was supported by the NSF CAREER Award No. 2042525, the Power Management Integration Center (PMIC) under the NSF IUCRC Award No. 2052809, and PMIC industry members. The authors would also like to thank Ryan Tran for his early efforts in power converter for motor drive and support in this research at the iPower3Es group.

REFERENCES

- [1] I. Aghabali et al, "800-V Electric Vehicle Powertrains: Review and Analysis of Benefits, Challenges, and Future Trends," *IEEE Transactions on Transportation Electrification*, vol. 7, no. 3, pp. 927–948, 2021.
- [2] C. K. Liu, "Novel High Power Density Turn-Less Motor Concept," Ph.D. dissertation, UC San Diego, 2018. [Online]. Available: <https://escholarship.org/uc/item/3gw1p047>
- [3] H. Zeng et al, "Modular Modeling and Distributed Control of Permanent-Magnet Modular Motor Drives (MMDs) for Electric Aircraft Propulsion," in *2021 ECCE*, 2021, pp. 4598–4605.
- [4] J. O. Estima et al, "Efficiency Analysis of Drive Train Topologies Applied to Electric/Hybrid Vehicles," *IEEE Transactions on Vehicular Technology*, vol. 61, no. 3, pp. 1021–1031, 2012.
- [5] T. M. Jahns et al, "The Incredible Shrinking Motor Drive: Accelerating the Transition to Integrated Motor Drives," *IEEE Power Electronics Magazine*, vol. 7, no. 3, pp. 18–27, 2020.
- [6] F. Wu, A. M. EL-Refaie, and T. M. Jahns, "Active Voltage Balancing of Integrated Modular Drive with Series DC-Link Capacitors," in *2020 ECCE*, 2020, pp. 1469–1476.
- [7] R. Das, G.-S. Seo, D. Maksimovic, and H.-P. Le, "An 80-W 94.6%-Efficient Multi-Phase Multi-Inductor Hybrid Converter," in *2019 APEC*, 2019, pp. 25–29.
- [8] L. Haokai and Y. Jian, "Research on inverter control system based on bipolar and asymmetric regular sampled SPWM," in *2013 IEEE 11th International Conference on Electronic Measurement & Instruments*, vol. 2, Aug. 2013, pp. 595–598.
- [9] R. Das and H.-P. Le, "Analysis of Capacitor Voltage Imbalance in Hybrid Converters and Inherently Balanced Operation Using Symmetric Architecture," *IEEE Journal of Emerging and Selected Topics in Industrial Electronics*, vol. 3, no. 4, pp. 1205–1209, Oct. 2022.
- [10] T. Habetler, R. Naik, and T. Nondahl, "Design and implementation of an inverter output LC filter used for dv/dt reduction," *IEEE Trans. on Pow. Elect.*, vol. 17, no. 3, pp. 327–331, 2002.
- [11] X. Ba et al, "Development of Equivalent Circuit Models of Permanent Magnet Synchronous Motors Considering Core Loss," *Energies*, vol. 15, no. 6, p. 1995, Jan. 2022.
- [12] Y. L. Juan, T. Rong Chen, S. M. Chen, L. Ling Chen, C. Y. Cheng, and S. Hsiang Hsiao, "Integrated Single-Stage Driver for BLDC Motors," in *2019 IEEE 4th International Future Energy Electronics Conference (IFEEC)*, Nov. 2019, pp. 1–4.